

RSC Advances



This is an *Accepted Manuscript*, which has been through the Royal Society of Chemistry peer review process and has been accepted for publication.

Accepted Manuscripts are published online shortly after acceptance, before technical editing, formatting and proof reading. Using this free service, authors can make their results available to the community, in citable form, before we publish the edited article. This *Accepted Manuscript* will be replaced by the edited, formatted and paginated article as soon as this is available.

You can find more information about *Accepted Manuscripts* in the [Information for Authors](#).

Please note that technical editing may introduce minor changes to the text and/or graphics, which may alter content. The journal's standard [Terms & Conditions](#) and the [Ethical guidelines](#) still apply. In no event shall the Royal Society of Chemistry be held responsible for any errors or omissions in this *Accepted Manuscript* or any consequences arising from the use of any information it contains.



New copper(II) complexes of anti-inflammatory drug mefenamic acid: a concerted study including synthesis, physicochemical characterization and their biological evaluation.

Received 00th January 20xx,
Accepted 00th January 20xx

DOI: 10.1039/x0xx00000x

www.rsc.org/

Raj Pal Sharma,^{a,*} Santosh Kumar,^a Paloth Venugopalan,^a Valeria Ferretti,^{b,*} Alketa Tarushi,^c George Psomas^{c*} and Maciej Witwicki^d

Reaction of hydrated copper(II) mefenamate in presence of diverse N-donor ligands such as N,N,N',N'-tetramethylethylenediamine (*temed*), ethylenediamine (*en*), β -picoline (*β -pic*) in methanol:water mixture (4:1, v/v) yielded crystalline monomeric copper(II) complexes [Cu(*temed*)(mefenamato)₂], **1**, [Cu(*en*)₂(H₂O)₂](mefenamato)₂, **2** and [Cu(*β -pic*)₂(mefenamato)₂]-H₂O, **3**. The newly synthesized complexes have been characterized by elemental analysis, spectroscopic methods (FT-IR, UV-Vis and EPR), thermogravimetric analyses and single-crystal X-ray structure determination in the case of complexes **2** and **3**. The ground-state geometry optimization of complex **1** was performed by DFT calculations. In order to verify the complexes capability to get bound and possibly transported by the albumin towards their biological targets (cells and/or tissues), the interaction with bovine (BSA) and human serum albumin (HSA) was studied by fluorescence emission spectroscopy. The interaction of complexes **1-3** with calf-thymus DNA (CT DNA) was monitored by UV-Vis spectroscopy, cyclic voltammetry, viscosity measurements and via the ethidium bromide (EB) displacement from the EB-DNA conjugate performed by fluorescence emission spectroscopy, as a preliminary approach to evaluate their potential biological activity.

Introduction

Non-steroidal anti-inflammatory drugs (NSAIDs) constitute an important class of compounds to alleviate inflammation and pain associated with disease or injury etc.; they exert their therapeutic effects by inhibiting the release of prostaglandin and thromboxane hormone produced in human body by enzymatic transformation.^[1-3] However, beyond certain limit, the use of NSAIDs is associated with various side effects such as kidney failure and gastrointestinal problems.^[4] Synthesis, physicochemical and structural investigations of metal complexes with active pharmaceuticals NSAIDs in which the drug molecules play a role of ligand when deprotonated (i.e., as anion) have been regarded as a research area of increasing interest for inorganic, pharmaceutical and medicinal chemistry.^[5] In comparison with NSAIDs, the metal centre in metal-NSAID complexes has possibility of different

^a Department of Chemistry, Panjab University, Chandigarh-160014, India.

^b Center for Structural Diffractometry and Department of Chemical and Pharmaceutical Sciences, University of Ferrara, via Fossato di Mortara 17-27, I-44121, Ferrara, Italy.

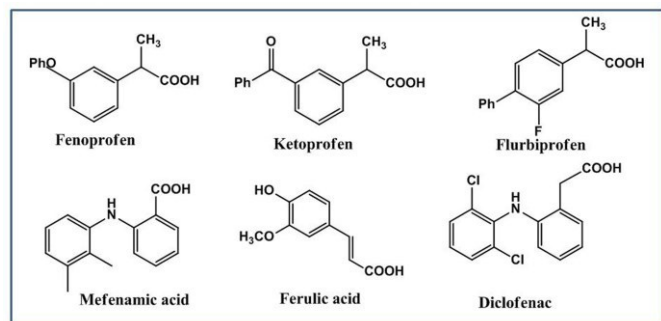
^c Department of General and Inorganic Chemistry, Faculty of Chemistry, Aristotle University of Thessaloniki, GR-54124 Thessaloniki, Greece.

^d Faculty of Chemistry, Wrocław University, 14 F. Joliot-Curie St., Wrocław 50-283, Poland

* Corresponding authors: rpsharmapu@yahoo.co.in (RPS), frt@unife.it (VF), gepsomas@chem.auth.gr (GP)

Supplementary Information (ESI) available: CCDC No. 1441703 (**2**) and 1441704 (**3**) contain the supplementary crystallographic data for this paper. These data can be obtained free of charge from The Cambridge Crystallographic Data Centre (12 Union Road, Cambridge, CB2 1EZ, UK) via www.ccdc.cam.ac.uk/data_request/cif. Available supplementary information: EPR, FT-IR, UV, and fluorescence spectra, cyclic voltammograms, Scatchard and Stern-Volmer quenching plots, interaction studies with CT DNA and serum albumins, competitive studies with EB. See DOI: 10.1039/x0xx00000x

coordination numbers, geometries and oxidation/reduction states that can be used to create structures which interact with target in unique ways. Moreover, these metal complexes may have lower toxicity and higher pharmaceutical effects as compared to free drug owing to the inhibition of metal complexation with other important biological compounds.^[6-8] Structural formulae of some common NSAIDs are given in Scheme 1.



Scheme 1. Structural formulae of some commonly used NSAIDs.

Most of the commonly used NSAIDs contain a carboxylic group (–COOH) which, when deprotonated, may exhibit a variety of coordination modes towards metal ions as shown in Fig. 1.

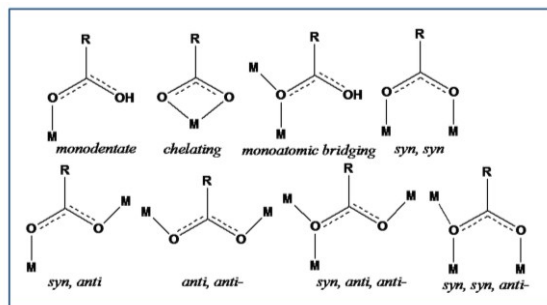


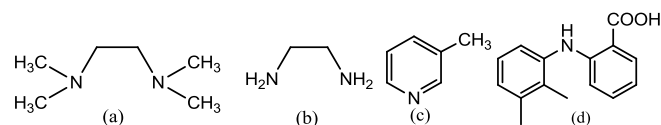
Fig. 1 Various possible coordination modes of carboxylate group in NSAIDs towards metal center. Out of these most commonly observed are monodentate (1), bidentate chelating (2) and bidentate bridging (all others).

Metal arylcarboxylates are among the most studied complexes due to their important biological properties.^[9-10] The combination of two or more different ligands into the same compound may bring multitargeted effects leading to synergistic action of the metal residue with dissociated molecular fragments from metal-NSAIDs inside the target tissue. In this direction, certain biometals such as copper might play an important role because of its presence in biological system and furthermore, copper(II) complexes with NSAIDs have been found to have more pronounced biological activities such as anti-bacterial, anti-cancer, DNA-binding, BSA-binding and DNA cleavage activities.^[11-15]

Judicious selection of mefenamic acid as complexing ligand (Hmef, 2-[(2,3-dimethylphenyl)-amino]-benzoic acid or N-(2,3-xilyl)anthranilic acid) is based on the fact that it is the most effective NSAID used in clinics because of its favourable anti-inflammatory and analgesic properties. On the other hand,

Hmef also exhibits some side-effects (headaches, diarrhea, vomiting and nervousness) similar to other NSAIDs.^[16-18] Its complexation with transition metal ions may reduce or diminish completely the side-effects. In this direction eventual isolation of copper(II) complexes with NSAIDs and successful lattice stabilization by exploiting the role of different non-covalent interactions necessitates the orientation of the interacting species (anions and cations) towards biomolecules. The mode of coordination of arylcarboxylate group towards a metal center can be altered to large extent by use of nitrogen-donor ligands. Moreover, nitrogen-donor ligands enhance the biological activities of transition metal complexes by altering coordination modes of other ligands towards metal center e.g. antitumor activity of the monomeric $[\text{Cu}(\text{asp})_2(\text{py})_2]$ is higher than dimeric $[\text{Cu}_2(\text{asp})_4]$, where pyridine is a nitrogen-donor ligand.^[19] In addition, nitrogen-donor ligands such as putrescine, spermine and spermidine occur in relatively higher concentration in the cells of all living organisms and take part in many biochemical processes.^[20]

To study the effect of different nitrogen-donor ligands, we have chosen, beside the mefenamate as carboxylate anion, the monodentate nitrogen-donor ligand β -picoline (β -pic) and the bidentate N-donor ligands ethylenediamine (*en*) and N,N,N',N'-tetramethylethylenediamine (*temed*) (Scheme 2).



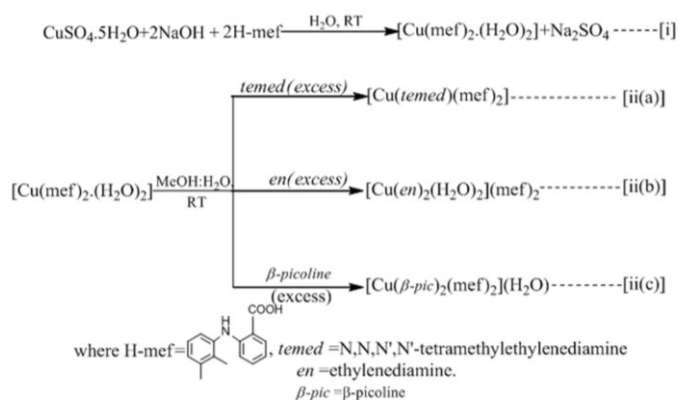
Scheme 2. Nitrogen-donor ligands used in present work: (a) *temed*, (b) *en*, (c) β -pic and (d) mefenamic acid.

The interaction of the resultant complexes with bovine (BSA) and human serum albumin (HSA) was studied in order to examine the possibility of such complexes to get bound and possibly transported by the albumins towards their biological targets (inflamed tissues and/or (cancer) cells, free radicals, DNA) in order to design target-specific drugs. As a part of our continuous interest in copper(II) complexes,^[21-24] we report herein, the synthesis, characterization and biological evaluation (interaction with BSA and HSA as well as with calf-thymus (CT) DNA) of three novel copper(II)-mefenamate complexes, i.e. $[\text{Cu}(\text{temed})(\text{mef})_2]$, **1**, $[\text{Cu}(\text{en})_2(\text{H}_2\text{O})_2](\text{mef})_2$, **2** and $[\text{Cu}(\beta\text{-pic})_2(\text{mef})_2]\cdot\text{H}_2\text{O}$, **3**.

Results and discussion

The hydrated copper(II) mefenamate was obtained by reacting hydrated copper sulfate with sodium salt of mefenamic acid as shown in Scheme 3 (eq. (i)). The precipitated product was then suspended in methanol-water mixture (4:1, v/v) followed by the addition of different nitrogen-donor ligands (*temed*, *en* and β -pic) with continuous stirring until a clear solution was observed in each case. Upon slow evaporation of respective resultant reaction mixtures at room temperature, three complexes **1**, **2** and **3** were isolated in good yields from

respective solutions as shown in Scheme 3 (equations (ii)-a-(ii)(c)).



Scheme 3. Schematic representation of the synthesis of complexes **1-3** i.e. $[\text{Cu}(\text{temed})(\text{mef})_2]$, **1**, $[\text{Cu}(\text{en})_2(\text{H}_2\text{O})_2](\text{mef})_2$, **2** and $[\text{Cu}(\beta\text{-pic})_2(\text{mef})_2]\cdot\text{H}_2\text{O}$, **3**.

The elemental analyses of newly synthesized complexes closely corresponded to structural formulae of monomeric copper(II) complexes $[\text{Cu}(\text{temed})(\text{mef})_2]$, **1**, $[\text{Cu}(\text{en})_2(\text{H}_2\text{O})_2](\text{mef})_2$, **2** and $[\text{Cu}(\beta\text{-pic})_2(\text{mef})_2]\cdot\text{H}_2\text{O}$, **3**, respectively. However, single-crystal X-ray structure determination of complexes **2** and **3** revealed the presence of different coordination modes of mefenamate ligand towards copper(II) ion in presence of different nitrogen-donor ligands resulting in different packing patterns in both complexes.

The newly synthesized complexes have been characterized by FT-IR and UV-vis spectroscopy. Infrared spectra of **1-3** were recorded in the region $4000\text{--}400\text{ cm}^{-1}$ and tentative bands assignments has been made on the basis of earlier reports in literature.^[25,26] In complex **1**, no significant broad peak was observed in the region $3500\text{--}3350\text{ cm}^{-1}$ indicating the absence of water molecules. The absorption band at 3585 cm^{-1} in complex **2** was assigned to O-H stretching vibration of coordinated water molecules to copper(II) centre. In complex **3**, absorption peak at 3217 cm^{-1} was assigned to O-H stretching vibration of water molecule. The sharp absorption peak at 3128 cm^{-1} for complex **2** was assigned to N-H stretching frequency of mefenamate or ethylenediamine ligands. The absorption bands in the region $3000\text{--}2900\text{ cm}^{-1}$ were assigned to $\text{C}(\text{sp}^2)\text{-H}$ stretching vibration. The absorption bands in the region $1630\text{--}1600\text{ cm}^{-1}$ were assigned to $\text{C}=\text{C}$ stretching vibration. In-plane deformation modes of NH group of mefenamate in the region $1650\text{--}1660$ and $1505\text{--}1510\text{ cm}^{-1}$ do not show any significant variation upon complexation with metal ion in all the complexes prepared as compared to the values in free anion indicated that NH group of mefenamate anion does not participate in bonding to copper(II) metal center.^[27,28] The sharp absorption peak at 1650 cm^{-1} observed in mefenamic acid disappeared on formation of sodium salt and two new bands appeared at 1612 cm^{-1} and 1373 cm^{-1} corresponding to $\nu_{\text{as}}(\text{COO})$ and $\nu_{\text{s}}(\text{COO})$ stretching vibrations of

carboxylate group.^[29,30] The parameter $\Delta\nu (= \nu_{\text{as}}(\text{COO}) - \nu_{\text{s}}(\text{COO}))$ is an important tool in assigning the mode of coordination of carboxylate ligand in metal-carboxylates. Amongst coordination modes of carboxylate coordination, i) ionic, ii) unidentate, iii) bidentate chelating are the most common. In complex **2**, the $\Delta\nu(\text{COO})$ value of 189 cm^{-1} falls in the range ($160 - 210\text{ cm}^{-1}$) observed for various ionic complexes e.g. sodium formate ($\Delta\nu = 201\text{ cm}^{-1}$), sodium acetate ($\Delta\nu = 164\text{ cm}^{-1}$), sodium mefenamate ($\Delta\nu = 190\text{ cm}^{-1}$) etc. The $\Delta\nu$ values of 254 cm^{-1} in complex **1** and 129 cm^{-1} in complex **3** indicated asymmetric bidentate as observed in $\text{Ph}_2\text{Sn}(\text{CH}_3\text{-COO})_2$; $\Delta\nu = 265\text{ cm}^{-1}$) and bidentate chelating coordination mode, respectively. The symmetric deformation vibrations of the $-\text{CH}_3$ group of mefenamate in complexes **1-3** were observed in the region $1300\text{--}1100\text{ cm}^{-1}$, while the absorption peaks observed in the region $1000\text{--}620\text{ cm}^{-1}$ might be assigned to in-plane bending and out-of-plane deformation vibrations of hydrogen atoms on aromatic rings. The absorption peaks observed around 500 cm^{-1} in complexes **1-3** are within the range reported for Cu-O and Cu-N stretching frequencies in the literature. The FT-infrared spectra for complexes **1-3** are shown in Fig. S1 of the Supporting Information.

Description of crystal structures and DFT calculations. The ORTEP diagrams of complexes **2** and **3** are given in Fig. 2 and 3, respectively. Selected bond lengths and bond angles are summarized in Table 1. Both structures crystallized in triclinic crystal system with P-1 space group; in both structures, the metal atoms lie on a symmetry centre. The coordination geometry around the copper in complex **2** can be described as elongated octahedral, the central atom being bonded to two chelating ethylenediamine ligands and two water molecules in apical position. The Cu-N/O bond distances agree well with those of similar reported complexes; in particular, the $\text{Cu-O}_{\text{aqua}}$ mean distance in octahedral diaquacopper complexes having the remaining position occupied by N-ligands is $2.49(1)\text{ \AA}$ (CSD search, 231 hits). The mefenamate anions are outside the Cu-first coordination sphere resulting into ionic complex formation.

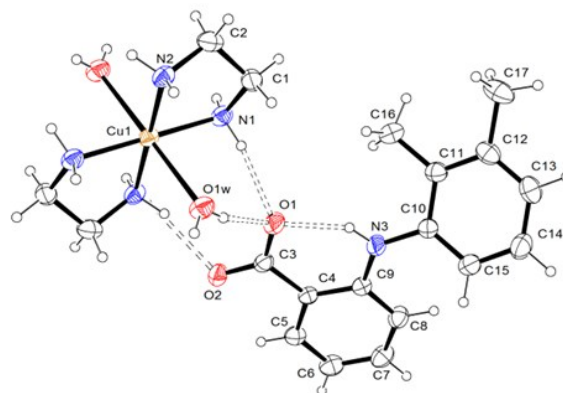


Fig. 2 ORTEP diagram and atom numbering scheme for the cation $[\text{Cu}(\text{en})_2(\text{H}_2\text{O})_2](\text{mef})^{1+}$ in complex **2**. Ellipsoids are drawn at 40% probability.

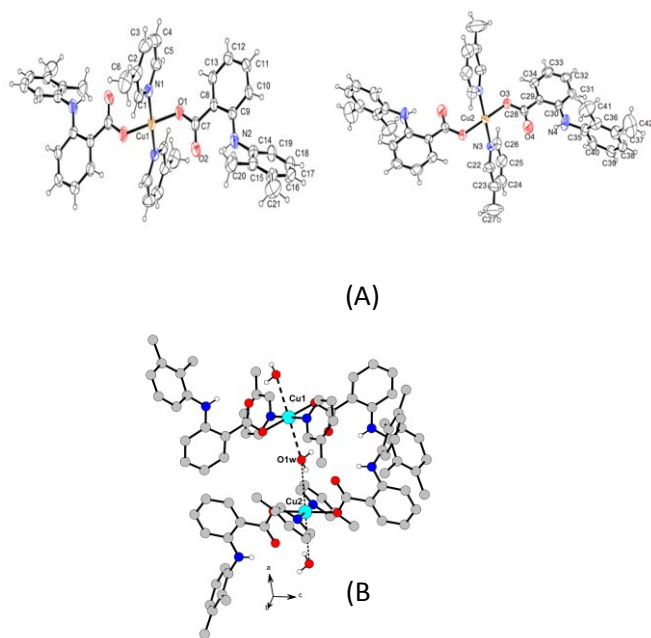


Fig. 3 (A) ORTEP diagram and atom numbering scheme of the two neutral coordination entities in complex **3** (in arbitrary orientation). The water molecule has been omitted for clarity. Ellipsoids are drawn at 40% probability; (B) the two complexes connected by the water molecule.

Table 1. Selected bond distances and angles (\AA , $^\circ$)

Complex 2		Complex 3	
Cu1 - N1	2.018(2)	Cu1 - N1	2.000(3)
Cu1 - O1W	2.494(2)	Cu1 - O1	1.938(3)
Cu1 - N2	2.015(2)	Cu2 - N3	2.031(6)
		Cu2 - O3	1.928(3)
N1-Cu1-O1W	85.77(7)	N1-Cu1-O1	88.6(1)
N1-Cu1-N2	84.75(8)	N1-Cu1-O1 ⁱ	91.4(1)
O1w-Cu- N1 ⁱ	94.28(7)	N3-Cu2-O3	89.7(2)
O1W-Cu1-N2	90.15(7)	N3-Cu2-O3 ⁱⁱ	90.3(2)
N1-Cu1-N2 ⁱ	95.26(8)		

Equivalent positions: (i) $-x, -y, 1-z$; (ii) $-x-1, -y, 1-z$

Conversely, in complex **3**, the asymmetric unit is formed by two half copper complexes, that are crystallographically independent, and a water molecule located at 2.670(4) and 3.037(4) \AA from the two central atoms Cu1 and Cu2, respectively (Fig. 3(B)). Each copper atom is linked to two β -picoline ligands and two mefenamate ligands coordinating in monodentate fashion. Due to the quite long Cu-Ow distances, in both cases the coordination geometry can be formally described as square planar; actually, taking into account only the basal ligands, the bond valence sum^[31] is 2.02 \AA and 1.96 \AA for Cu1 and Cu2, respectively.

In both complexes **2** and **3**, the crystal architecture is dominated by the formation of N/O-H...O hydrogen bonds. In complex **2**, the scarceness of good H-bond acceptor groups in combination with the profusion of H-bond donors makes possible the formation of bi- or trifurcated hydrogen-bonding interactions (as an example, see Fig. 2). Actually, each aqua ligand as well as the $-\text{NH}_2$ or $-\text{NH}$ groups act as donors in intra-

and intermolecular O/N-H...O bonds towards the oxygen atoms of the carboxylate group in mefenamate. The overall structure is made of organic/inorganic layers parallel to the b direction; besides O-H...O and N-H...O hydrogen-bonds, (see Table S1 of the Supplementary Information) it is stabilized also by N-H... π interactions with a H...Centroid (C4-C9) distance of 2.70 \AA and a N1-H...Centroid angle of 146 $^\circ$ (Fig. S2).

Conversely, in complex **3** the characteristic feature of the packing pattern is the formation of chain as shown in Fig. S3. The free water molecule joins the adjacent neutral copper complexes not only through Ow...metal short contacts, but also *via* the formation of Ow-H...O hydrogen bonds involving the non-coordinated carboxylate oxygen. The junction of the molecules in the chain is made tighter by strong N-H...O interactions (Table S1).

The crystals of complex **1** appeared good but did not diffract X-rays. Therefore, to find out a plausible structure for complex **1**, DFT calculations were carried out. It was disclosed that the molecular structure of complex **1** is expected to be strongly distorted (see dihedral angles in Fig. 4) but the distances between Cu and axial oxygen atoms are longer than those between the central metal ion and any equatorial donor atom. As can be expected for such a structure of Cu(II) complex, the unpaired electron occupies a molecular orbital with significant contribution of the $3d_{x^2-y^2}$ atomic orbital of copper.

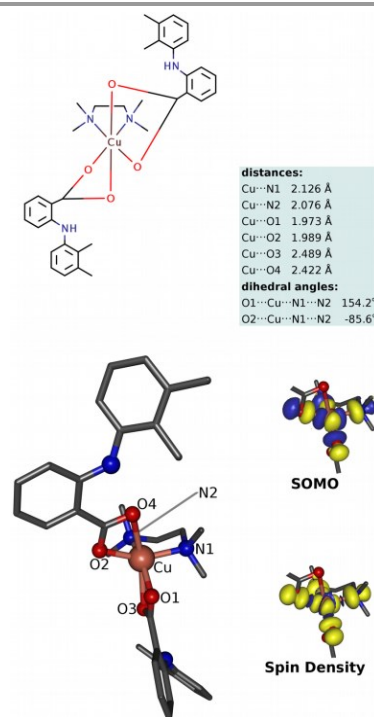


Fig. 4 Structure, singly occupied molecular orbital (SOMO) and spin density iso surfaces of complex **1**. All predicted at the ZORA/UB3LYP/def2-TZVP level. Hydrogen atoms were removed for clarity.

Coordination behaviour of mefenamate ligand towards copper(II) centre in presence of different nitrogen-donor ligands to form complexes **1-3** was further investigated by EPR spectroscopy.

EPR Spectroscopy. According to the elemental analysis (see Experimental section) complex **1** incorporates two mefenamate ligands and one *temed* ligand and, therefore, Cu(II) is expected to be coordinated to two nitrogen and two oxygen donor atoms. X- and Q-band EPR spectra of powdered complex **1** (Fig. S4) revealed $g_1 = 2.178$, $g_2 = 2.155$, and $g_3 = 2.035$. The shape of the signals at the particular g-components might imply their reverse relation (an indication of compressed octahedral and $\{d_{z^2}\}^1$ ground state) and the observed value of g_1 is relatively close to 2.0 as expected in such a case.^[32,33] However, the value of g_1 is dramatically lower than the ones known for the Cu(II) complexes with two N and two O donor atoms.^[34] This fact indicates that the observed g-components result from the coupling of g-tensors from coordination polyhedra non-parallel aligned in the crystal structure of complex **1** and, therefore, they are likely to sharply differ from the molecular g_x , g_y and g_z values.^[35,36] This interpretation stays in line with the molecular structure and $\{d_{x^2-y^2}\}^1$ ground state predicted by DFT. In addition, the g-components were calculated at the ZORA/UB3LYP/def2-TZVP theory level and these theoretical values ($g_x = 2.201$, $g_y = 2.064$, and $g_z = 2.062$) are a characteristic of Cu(II) complex with a $\{d_{x^2-y^2}\}^1$ ground state.

The EPR spectra of powdered complex **2** are typical for axial symmetry of Cu(II) coordination polyhedron with a limited rhombic distortion ($g_z = 2.221$, $g_y = 2.052$, and $g_x = 2.047$). This stays in line with the structure of complex **2** determined from the X-Ray diffraction experiment. Although complex **3** may be considered as Cu(II) dimer with the two Cu(II) cations bridged by a water molecule, the EPR spectra of complex **3** clearly indicate that it is not an exchange coupled system. The lack of exchange coupling is most likely due to relatively large distance between the Cu(II) ions, that is 5.648 Å. It is worth to emphasize that EPR spectra of complex **3** reveal not only the g-parameters ($g_x = 2.280$, $g_y = 2.067$, and $g_z = 2.058$) but also hyperfine coupling; approximately $a_z(\text{Cu}) = 170$ Gauss.

Conductance measurements. Conductance measurements of complex **2** were carried out at 25 °C in aqueous medium and a plot of K (molar conductance) versus $C^{1/2}$ (square root of concentration) was drawn. When the concentration was extrapolated to zero, it gave $\Lambda_0 = 238 \text{ S.cm}^2.\text{mol}^{-1}$. This value falls in the range observed for 1:2 electrolytes.^[37] Therefore, conductance measurements revealed that complex **2** behaves as 1:2 electrolyte in aqueous medium supporting ionic formulation of this complex i.e. $[\text{Cu}(\text{en})_2(\text{H}_2\text{O})_2](\text{mefenamato})_2$. A plot of K (molar conductance) versus $C^{1/2}$ (square root of concentration) is shown in Fig. S5. For complexes **1** and **3**, conductance measurements were not performed as these complexes are covalent in nature and do not dissociate in aqueous medium and other polar solvents.

Thermogravimetric analyses. Thermogravimetric studies of complexes **1-3** were performed under nitrogen atmosphere to study the stability of the complexes at elevated temperature. There is no stable peak observed in the Thermogravimetric curves for all the complexes **1-3**. The temperature range from 120 °C to 270 °C corresponds to loss of water molecules in complexes **2** and **3**. Thereafter, no significant stabilization in TGA plot has been observed for complex **1** corresponding to loss of both the organic ligands gradually even up to 1000 °C. Thermogravimetric stabilization was observed for complexes **2**

and **3**, i.e. after 400 °C for complex **2** and after 300 °C for complex **3** corresponding to formation of stable cupric oxide in both cases. TGA plots for complexes **1-3** have been given in Fig. 5.

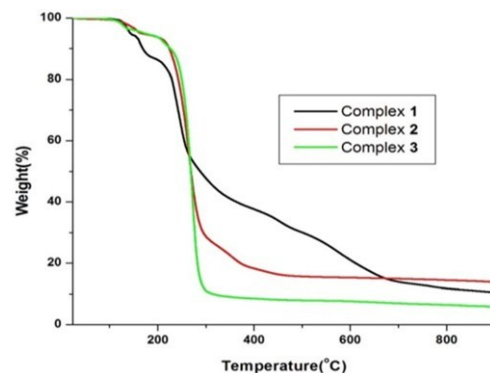


Fig. 5 Thermo-gravimetric analyses plots of complexes **1-3**.

Biological activity: Interaction of the complexes with CT DNA.

The structure of the metal complexes and the nature as well as lability of the bound ligands are the most important factors that may affect the interaction mode between the complexes and double-stranded DNA. More specifically, one or more labile ligands may be replaced by a nitrogen atom of DNA-base leading to covalent binding to DNA. In the case of complexes that keep their structure and integrity in solution, cleavage of the DNA-helix or non-covalent to DNA (i.e. intercalation, electrostatic interaction or groove-binding) may occur.^[38] So as to evaluate the effect of complexes **1-3** to CT DNA, their interaction was investigated by UV-Vis spectroscopy, cyclic voltammetry and viscosity measurements. Furthermore, the EB-displacing ability of the complexes was monitored by fluorescence emission spectroscopy.

Study of the DNA-interaction with complexes 1-3 by UV-Vis spectroscopy. UV-Vis spectroscopy is a technique able to provide information in regard to the DNA-binding mode and the strength of the complexes. Therefore, the UV-Vis spectra of a CT DNA solution ($1.2\text{-}1.5 \times 10^{-4} \text{ M}$) were recorded in the presence of complexes **1-3** at increasing amounts (for different r values) as well as the UV spectra of the complexes ($3\text{-}5 \times 10^{-5} \text{ M}$) in the presence of CT DNA at increasing amounts. Any changes of the CT DNA band at 257-260 nm or the intra-ligand transition bands of the complexes during the corresponding spectrophotometric titrations may reveal such interaction and provide useful information in regard to the interaction.^[39]

The UV-Vis spectra of a CT DNA solution in the presence of complex **3** at increasing r values are shown representatively in Fig. 6(A). The observed slight decrease of the absorbance at $\lambda_{\text{max}} = 257 \text{ nm}$ shows the existence of interaction between CT DNA and the complex which results in the formation of a new conjugate between complex **3** and CT DNA. Quite similar is the behaviour of CT DNA in the presence of complexes **1** and **2** (data not shown).

In the UV-Vis spectrum of complex **3** ($5 \times 10^{-5} \text{ M}$) (Fig. 6(B)), the band centred at 343 nm (band I) exhibits a significant hypochromism of ca. 30% suggesting tight binding to CT DNA probably by intercalation attributed to $\pi \rightarrow \pi$ stacking interaction between the aromatic chromophores from the ligands and DNA-base pairs.^[39] The band shows initially a slight

blue-shift and is gradually eliminated with further addition of DNA. Additionally, the band at 288 nm (band II) presents a hyperchromism of up to 25% accompanied by a red-shift of 9 nm (up to 297 nm), suggesting tight binding and stabilization. A distinct isobestic point at 333 nm appears upon addition of CT DNA. The behaviour of complexes **1** and **2** upon addition of increasing amounts of CT DNA (Fig. S6) is similar with less pronounced hypo-/hyper-chromic effects (Table 2). Such behaviour of metal-mefenamato complexes in the presence of a CT DNA solution was previously observed for Co(II), Cu(II), Zn(II) and Ni(II) mefenamato complexes with heterocyclic N,N'-donors as co-ligands.^[40-43]

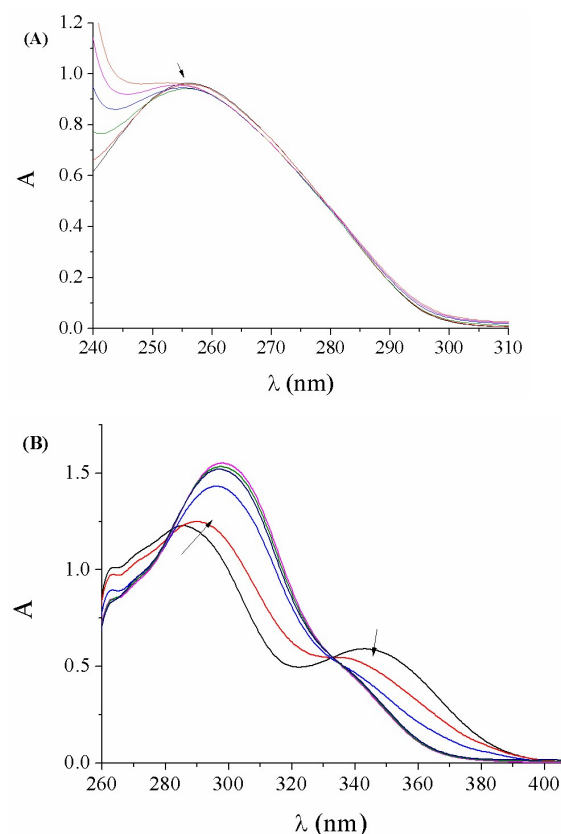


Fig. 6 (A) UV-Vis spectra of CT DNA (1.45×10^{-4} M) in buffer solution (150 mM NaCl and 15 mM trisodium citrate at pH 7.0) in the absence or presence of complex **3**. The arrow shows the changes upon increasing amounts of the complex. (B) UV-Vis spectra of DMSO solution of complex **3** (5×10^{-5} M) in the presence of increasing amounts of CT DNA ($r = [\text{DNA}]/[\text{compound}] = 0-0.8$). The arrows show the changes upon increasing amounts of CT DNA.

Table 2. UV-Vis spectral features of the interaction of Hmef and its complexes **1-3** with CT DNA; UV-band (λ , nm) (percentage of the observed hyper-/hypo-chromism ($\Delta A/A_0$, %), blue-/red-shift of the λ_{max} ($\Delta\lambda$, nm)) and DNA-binding constants (K_b).

Compound	Band ($\Delta A/A_0$ ^a , $\Delta\lambda$ ^b)	K_b (M^{-1})
Hmef [43]		$1.05(\pm 0.02) \times 10^5$
1	338 (-19.0 ^a , 0) 296 (+6.0 ^a , +5 ^b)	$1.17(\pm 0.13) \times 10^6$
2	340 (-8.0, 0) 292 (+10.0, +3)	$5.37(\pm 0.25) \times 10^5$
3	343 (-30.0, -3 ^b) 288 (+25.0, +9)	$1.90(\pm 0.12) \times 10^6$

^a "+" denotes hyperchromism, "-" denotes hypochromism

^b "+" denotes red-shift, "-" denotes blue-shift

The DNA-binding constants (K_b) of complexes **1-3** (Table 2) were determined by the Wolfe-Shimer equation^[44] (eq. S1) and the plots $[\text{DNA}]/(\epsilon_A - \epsilon_f)$ versus $[\text{DNA}]$ (Fig. S7). In brief, the complexes have relatively high K_b constants which are higher than free Hmef suggesting their tight binding to CT DNA. The K_b constants are also higher than that of the classical intercalator EB ($= 1.23(\pm 0.07) \times 10^5 \text{ M}^{-1}$) as calculated by Psomas and Kessissoglou.^[45] Complex **3** has the highest K_b constant ($= 1.90(\pm 0.12) \times 10^6 \text{ M}^{-1}$) among the present compounds which is the second highest K_b value among the metal-mefenamato complexes reported so far^[40-43] and is among the strongest DNA-binders when compared to the previously reported metal-NSAID complexes.^[46-53]

The existing findings from the UV-Vis spectroscopy experiments may suggest that the complexes can bind tight to CT DNA and observed hypochromic effect may be considered as first evidence of probable intercalation of the complexes to CT DNA.^[39,54] Despite that and as it is known, the exact mode of DNA-binding cannot be definitely concluded by UV-Vis spectroscopic titration studies but more experiments including cyclic voltammetry, viscosity measurements and EB-displacing studies were conducted to better clarify the interaction mode.

Study of DNA-interaction with complexes 1-3 by cyclic voltammetry. Cyclic voltammetry is a complimentary technique that may provide useful information concerning the DNA-interaction mode of metal ions or complexes.^[55] The cyclic voltammograms of the complexes in a 1/2 DMSO/buffer solution were recorded in the absence and presence of CT DNA (Fig. S8). No new redox peaks appeared suggesting that there is equilibrium between free and DNA-bound complex.^[55] The cathodic (E_{pc}) and anodic (E_{pa}) potentials of the redox couple Cu(II)/Cu(I) for each complex as well as their shifts upon addition of CT DNA are given in Table 3.

Table 3. Cathodic and anodic potentials (in mV) for the redox couple Cu(II)/Cu(I) of complexes **1-3** in 1/2 DMSO/buffer solution in the absence or presence of CT DNA.

Complex	$E_{\text{pc}(f)}$ ^a	$E_{\text{pc}(b)}$ ^b	ΔE_{pc} ^c	$E_{\text{pa}(f)}$ ^a	$E_{\text{pa}(b)}$ ^b	ΔE_{pa} ^c
1	-735	-695	+40	-480	-475	+5
2	-765	-735	+30	-415	-465	-50
3	-725	-715	+10	-495	-485	+10

^a $E_{\text{pc/a}}$ in DMSO/buffer in the absence of CT DNA ($E_{\text{pc/a}(f)}$)

^b $E_{\text{pc/a}}$ in DMSO/buffer in the presence of CT DNA ($E_{\text{pc/a}(b)}$)

^c $\Delta E_{\text{pc/a}} = E_{\text{pc/a}(b)} - E_{\text{pc/a}(f)}$

Upon addition of CT DNA, the cathodic and the anodic potentials of complexes **1** and **3** exhibit a positive shift ($\Delta E_{\text{pc/a}} = (+5)-(+40)$ mV) leading to the conclusion that intercalation is the most possible mode of interaction between the complexes and CT DNA,^[48-51, 56] a conclusion which is in agreement with the viscosity experiments and supports the UV spectroscopic findings. For complex **2**, the cathodic potential shows a positive shift ($\Delta E_{\text{pc}} = +30$ mV), indicating interaction via intercalation, while the anodic potential exhibited a negative shift ($\Delta E_{\text{pa}} = -50$ mV) revealing the electrostatic interaction of complex **2** with DNA which may be expected for dicationic complex **2**^[56,57] since cationic complexes usually interact with anionic phosphate groups of the DNA duplex; thus, for

complex **2** we may suggest the co-existence of external (electrostatic) interaction and intercalation.^[56]

Study of the DNA-interaction with complexes 1-3 by viscosity measurements. The DNA-viscosity is sensitive to the DNA-length changes in the presence of a DNA-binder since the relative DNA-viscosity (η/η_0) is connected with relative DNA-length (L/L_0) via the equation $L/L_0 = (\eta/\eta_0)^{1/3}$.^[58,59] In general, the DNA-viscosity enhances when the DNA-length increases as a result of separation distance of the DNA bases in order to host an intercalating compound. In the case of non-classic intercalation (i.e. external interaction such as electrostatic interaction or groove-binding), the DNA-bases separation distance remains almost stable; as a result of such interaction a bend or kink of the DNA-helix may occur followed by a slight decrease of DNA-length and subsequently the DNA-viscosity will be slightly affected or even decreased.^[47-53, 56]

The DNA-viscosity measurements were carried out on CT DNA solutions (0.1 mM) in the presence of increasing amounts of complexes **1-3** (up to the value of $r = 0.35$, Fig. 7). In the presence of complexes **1-3** and up to $r = 0.1$, the DNA-viscosity remained almost stable; for further addition of the complexes ($r > 0.1$), a considerable increase of the relative DNA-viscosity was observed. Such behaviour indicates initially ($r \leq 0.1$) the interaction of the complexes via non-classical intercalation, especially electrostatic interaction for complex **2**, which is followed by intercalation of each complex between the DNA-bases. Such conclusions are in good agreement with the findings from cyclic voltammetry experiments.

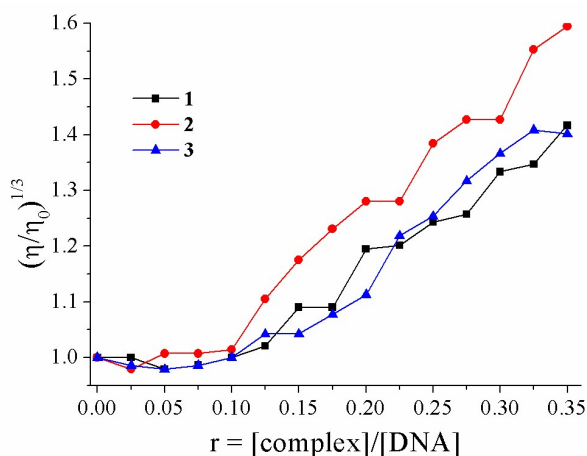


Fig. 7 Relative viscosity (η/η_0)^{1/3} of CT DNA (0.1 mM) in buffer solution (150 mM NaCl and 15 mM trisodium citrate at pH 7.0) in the presence of complexes **1-3** at increasing amounts ($r = [\text{compound}]/[\text{DNA}]$).

Study of the DNA-interaction of the complexes by ethidium bromide-displacement. The ability of complexes **1-3** to displace ethidium bromide (EB) from the EB-DNA conjugate may further verify their intercalating ability. The classic DNA-intercalator EB intercalates to CT DNA via its planar phenanthridine ring with the resultant EB-DNA conjugate exhibiting an intense fluorescence emission band at 592 nm, when excited at 540 nm.^[60, 61] The complexes did not show any fluorescence emission bands at room temperature in solution or in the presence of CT DNA or EB under the same experimental conditions ($\lambda_{\text{exc}} = 540$ nm). Thus, it was possible

to monitor the competition between the complexes and EB for the intercalation sites of DNA by fluorescence emission spectroscopy with $\lambda_{\text{exc}} = 540$ nm.

A solution of EB ($[\text{EB}] = 20 \mu\text{M}$) was pre-treated with DNA ($[\text{DNA}] = 26 \mu\text{M}$) in order to form the EB-DNA conjugate. Thus, the fluorescence emission spectra ($\lambda_{\text{exc}} = 540$ nm) of EB-DNA were recorded in the presence of increasing amounts of complexes **1-3** up to the r value of 0.24 (representatively shown for complex **3** in Fig. 8(A)). The addition of the compounds resulted in a significant decrease of the intensity (Fig. 8(B)) of the emission band of the EB-DNA system at 592 nm (the final quenching is up to 79.8% of the initial EB-DNA fluorescence intensity, Table 4) which verified the competition of the complexes with EB in binding to DNA. The significant quenching of EB-DNA fluorescence by the complexes may reveal the ability of the complexes to displace EB from the EB-DNA conjugate and may indirectly indicate that the complexes may bind to CT DNA possible by an intercalative mode.^[62]

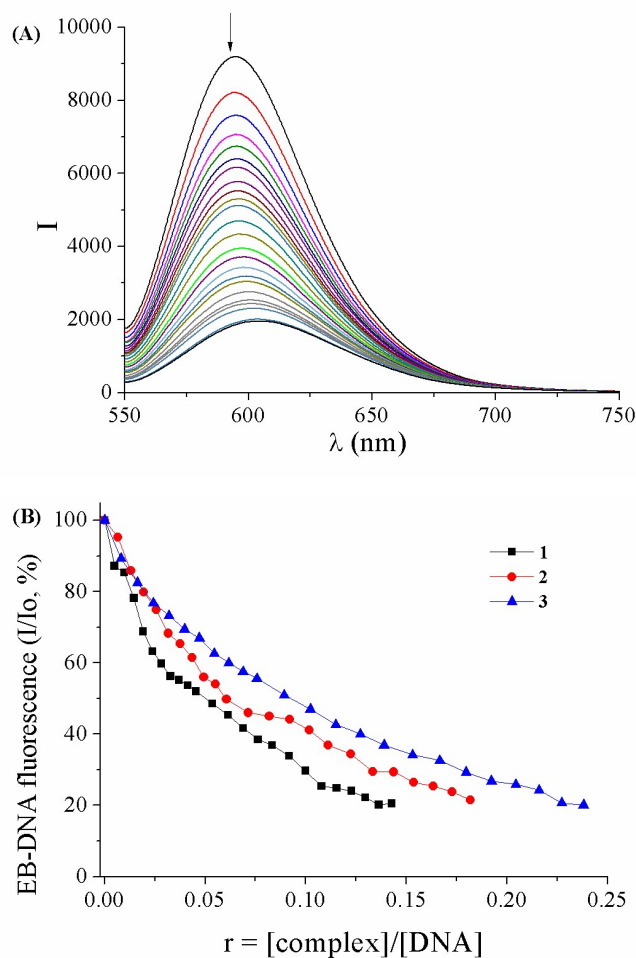


Fig. 8 (A) Fluorescence emission spectra ($\lambda_{\text{exc}} = 540$ nm) for EB-DNA ($[\text{EB}] = 20 \mu\text{M}$, $[\text{DNA}] = 26 \mu\text{M}$) in buffer solution in the absence and presence of increasing amounts of complex **3** (up to the value of $r = 0.25$). The arrow shows the changes of intensity with increasing amounts of **3**. (B) Plot of relative EB-DNA fluorescence emission intensity (I/I_0 , %) at $\lambda_{\text{em}} = 592$ nm vs $r (= [\text{complex}]/[\text{DNA}])$ in buffer solution (150 mM NaCl and 15 mM trisodium citrate at pH 7.0) in the presence of complexes **1-3** (up to 20.5% of the initial EB-DNA fluorescence for **1**, 21.5% for **2** and 20.2% for **3**).

Table 4. Percentage of EB-DNA fluorescence quenching at $\lambda_{em}=592$ nm ($\Delta I/I_0$, %) and Stern-Volmer constants (K_{SV}).

Compound	$\Delta I/I_0$ (%)	K_{SV} (M^{-1})
Hmef [43]	80.0	$1.58(\pm 0.06) \times 10^5$
1	79.5	$3.75(\pm 0.08) \times 10^5$
2	78.5	$3.02(\pm 0.06) \times 10^5$
3	79.8	$2.11(\pm 0.04) \times 10^5$

The Stern-Volmer plots of the EB-DNA fluorescence (Fig. S9) may confirm that the complexes induce the quenching of the EB-DNA fluorescence in good agreement ($R = 0.99$) with the linear Stern-Volmer equation (eq. S2); thus, the quenching may be considered a result of the displacement of EB from EB-DNA conjugate by the complexes.^[62] The K_{SV} constants of the complexes (Table 4) were calculated by the Stern-Volmer equation (eq. S2), are relatively high verifying tight binding to DNA and are within the range reported for other metal-NSAIDs complexes.^[45-52] The complexes have higher K_{SV} constants than free Hmef, with complex **1** bearing the highest K_{SV} constant ($= 3.75(\pm 0.08) \times 10^5 M^{-1}$) among complexes **1-3**.

Interaction of complexes 1-3 with serum albumins. The role of the serum albumins (SAs) is the transfer of ions and drugs through the bloodstream towards their biological targets, i.e. cells, tissues and free radicals.^[60,52d] Thus, the interaction of SAs with compounds of tentative biological interest (such as complexes **1-3** in the present case) should be studied as a first evaluation of the biological activity; during such binding, the biological properties of the system may change or novel possible transportation mechanisms may occur.^[63] Within this context, the study of complexes **1-3** interacting with two SAs (HSA and BSA which, as homologue of HSA, is the most studied SA) was performed. The solution of albumins exhibits an intense fluorescence emission, with excitation wavelength at 295 nm, which is attributed to the existence of tryptophans. In particular, HSA with a tryptophan at position 214 presents an emission band at $\lambda_{em,max} = 352$ nm while BSA has two tryptophans at positions 134 and 212 with $\lambda_{em,max} = 343$ nm.^[60] In addition, the inner-filter effect was calculated with eq. S3, was too low and may not affect the measurements.^[64]

The fluorescence emission spectra of HSA exhibited in the presence of complexes **1-3** a significant quenching of the fluorescence (quenching of the initial HSA fluorescence emission is up to ca. 84.3%) while the quenching observed in the fluorescence emission spectra of BSA was much more pronounced (up to ca. 97.7% of the initial BSA fluorescence) (Fig. S10 and Fig. 9). Thus, the addition of complexes **1-3** in a SA solution may induce a significantly high quenching which may be assigned to changes of the SA-tryptophan environment due to SA secondary structure changes resulted from the binding of the complexes to the albumins.^[65]

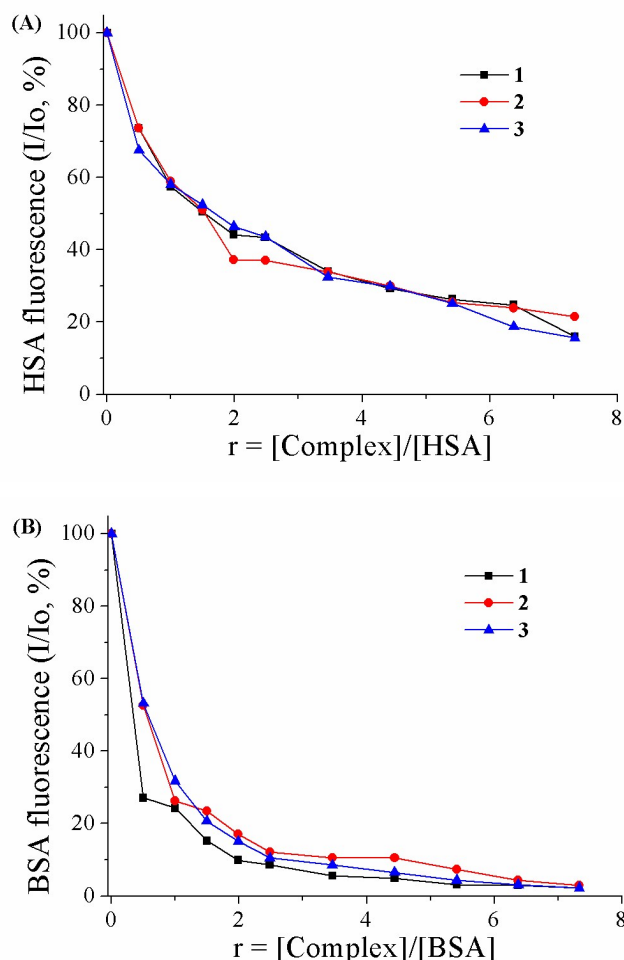


Fig. 9 (A) Plot of relative HSA-fluorescence intensity at $\lambda_{em} = 352$ nm (I/I_0 , %) vs r ($r = [\text{complex}]/[\text{HSA}]$) for complexes **1-3** (up to 16.0% of the initial HSA fluorescence for complex **1**, 21.5% for **2** and 15.7% for **3**) in buffer solution (150 mM NaCl and 15 mM trisodium citrate at pH 7.0). (B) Plot of relative BSA-fluorescence intensity at $\lambda_{em} = 343$ nm (I/I_0 , %) vs r ($r = [\text{complex}]/[\text{BSA}]$) for complexes **1-3** (up to 2.3% of the initial BSA fluorescence for complex **1**, 3.0% for **2** and 2.4% for **3**) in buffer solution (150 mM NaCl and 15 mM trisodium citrate at pH 7.0).

The quenching constants (k_q) for the interaction of the compounds with SAs were calculated with the Stern-Volmer quenching equation (eqs. S4 and S5) using the corresponding Stern-Volmer plots (Fig. S11 and S12) and their values are cited in Table 5. The k_q constants show the significant SA-quenching ability for the complexes and they are significantly higher than $10^{10} M^{-1}s^{-1}$ suggesting that the quenching takes place via a static mechanism.^[66] The k_q constants of the complexes are higher than those of free Hmef, with complex **1** showing the highest k_q constant for BSA and complex **3** for HSA. The derived k_q constants are within the range found for a series of metal-complexes bearing NSAIDs as ligands.^[31-43,47-53]

Table 5. The albumin constants for complexes **1-3**.

Compound	k_a ($M^{-1}s^{-1}$)	K (M^{-1})
BSA		
Hmef [43]	$2.78(\pm 0.20) \times 10^{13}$	1.35×10^5
1	$1.91(\pm 0.09) \times 10^{14}$	$1.80(\pm 0.07) \times 10^6$
2	$1.19(\pm 0.06) \times 10^{14}$	$5.63(\pm 0.16) \times 10^5$
3	$1.40(\pm 0.06) \times 10^{14}$	$5.32(\pm 0.22) \times 10^5$
HSA		
Hmef [43]	$7.13(\pm 0.34) \times 10^{12}$	1.32×10^5
1	$1.65(\pm 0.05) \times 10^{13}$	$2.85(\pm 0.11) \times 10^5$
2	$1.62(\pm 0.05) \times 10^{13}$	$2.72(\pm 0.07) \times 10^5$
3	$2.35(\pm 0.09) \times 10^{13}$	$1.97(\pm 0.09) \times 10^5$

The values of K constants of complexes **1-3** (Table 5) were determined with the Scatchard equation^[67] (eq. S6) using the Scatchard plots (Fig. S13 and Fig. S14). The K constants of the complexes are relatively high and similar to those calculated for a series of metal complexes with NSAIDs as ligands.^[41-43,47-53] In general, the complexes exhibit higher affinity for the albumins than free Hmef with complex **1** exhibiting the highest affinity for BSA and the lowest affinity for HSA among the complexes (Table. 5)

The K constants of complexes **1-3** are in the range 1.97×10^5 - $1.80 \times 10^6 M^{-1}$ and are relatively high, showing the tentative ability of the complexes to bind to SAs so as to get transported by them towards their biological targets such as cells or tissues. Additionally, they are significantly lower than the value of $10^{15} M^{-1}$ (this is the value of the association constant of diverse compounds with avidin which are considered among the strongest known non-covalent interaction^[68]) showing that the compounds are reversibly bound to the SAs and may get released when they arrive at their biological targets.^[65]

Conclusions

The three novel copper(II)-mefenamate complexes, $[Cu(\textit{temed})(\textit{mef})_2]$, **1**, $[Cu(\textit{en})_2(\textit{H}_2\textit{O})_2](\textit{mef})_2$, **2** and $[Cu(\beta\textit{-pic})_2(\textit{mef})_2] \cdot \textit{H}_2\textit{O}$, **3** have been characterized by diverse physico-chemical studies and single-crystal X-ray crystallography. The interaction of these complexes **1-3** with CT DNA was monitored by diverse techniques (UV-Vis spectroscopic methods, viscosity measurements, cyclic voltammetry and EB-displacing studies) which revealed the ability of the complexes to bind to CT DNA, probably via intercalation. Based on the DNA-binding constants, complex **3** is among the strongest DNA-binders when compared to the previously reported metal-NSAID complexes. The BSA- and HAS-binding constants of complexes **1-3** suggest not only that they can bind to these albumins so as to get transferred by them, but also that they may get released when they arrive at their biological targets.

Experimental

Material and Physical measurements

Analytical grade reagents were used throughout this work without any further purification. C, H and N were estimated micro analytically by automatic Perkin Elmer 2400 CHN

element analyzer and copper was determined by standard literature methods.^[69,70] Fourier transform infrared spectra were recorded on Perkin Elmer Spectrum RX FT-IR system in solid state. UV-visible (UV-Vis) spectra were recorded using Hitachi 330 Spectrophotometer or a Hitachi U-2001 dual beam spectrophotometer. The EPR spectra at 9.6 GHz (X-band) and 34 GHz (Q-band) were measured at 77 K and 100 K, respectively, using a Bruker Elexsys E500 spectrometer equipped with a NMR teslameter and frequency counter. The simulations of the experimental spectra were performed using a computer program employing full diagonalization of the spin Hamiltonian matrix, written by Dr. A. Ozarowski (National High Magnetic Field Laboratory, Florida State University). All the theoretical calculations were carried out with the ORCA 3.0.3 suite of programs^[71] using the UB3LYP^[72-74] hybrid functional, together with the ZORA^[75] method for the scalar relativistic effects and the def2-TZVP basis set in its scalar relativistic variant.^[76] The g-tensor calculations were performed using Neese's coupled perturbed Kohn-Sham method.^[77,78] The RIJCOSX approximation^[79] was used only for geometry optimizations, hence in these calculations the appropriate auxiliary basis set was employed. Each of the stationary points was fully characterized as a true minimum through vibrational analysis.

CT DNA, HSA and BSA were purchased from Sigma-Aldrich Co. and the solvents were purchased from Merck. All the chemicals and solvents were reagent grade and were used as purchased.

DNA stock solution was prepared by dilution of CT DNA by buffer (containing 15 mM trisodium citrate and 150 mM NaCl at pH 7.0) followed by exhaustive stirring for three days, and kept at 4°C for no longer than two weeks. The stock solution of CT DNA gave a ratio of UV absorbance at 260 and 280 nm (A_{260}/A_{280}) of 1.87, indicating that the DNA was sufficiently free of protein contamination.^[80] The DNA concentration was determined by the UV absorbance at 260 nm after 1:20 dilution using $\epsilon = 6600 M^{-1}cm^{-1}$.^[81] UV-visible (UV-vis) spectra were recorded on a Hitachi U-2001 dual beam spectrophotometer. Fluorescence spectra were recorded in solution on a Hitachi F-7000 fluorescence spectrophotometer. Viscosity experiments were carried out using an ALPHA L Fungilab rotational viscometer equipped with an 18 mL LCP spindle and the measurements were performed at 100 rpm.

Cyclic voltammetry studies were performed on an Eco chemieAutolab Electrochemical analyzer. Cyclic voltammetric experiments were carried out in a 30 mL three-electrode electrolytic cell. The working electrode was platinum disk, a separate Pt single-sheet electrode was used as the counter electrode and a Ag/AgCl electrode saturated with KCl was used as the reference electrode. The cyclic voltammograms of the complexes in the presence of CT DNA were recorded in 0.4 mM 1/2 DMSO/buffer solutions at $v = 100 mV s^{-1}$ where the buffer solution was the supporting electrolytes. Oxygen was removed by purging the solutions with pure nitrogen which had been previously saturated with solvent vapors. All electrochemical measurements were performed at 25.0 ± 0.2 °C.

Synthesis of $[Cu(\textit{temed})(\textit{mef})_2]$, 1. $CuSO_4 \cdot 5H_2O$ (0.50 g, 2 mmol) was dissolved in 10 mL of distilled water. Sodium salt of mefenamic acid was prepared *in situ* by dissolving NaOH (0.16 g, 4 mmol) and Hmef (0.99 g, 4 mmol) in the minimum amount

of water. On mixing the two solutions, precipitated product of copper(II) mefenamate resulted immediately. The precipitated product was filtered through a fine filter paper, washed with water followed by methanol and dried at room temperature (yield 85 %). Copper(II) mefenamate was then suspended in methanol-water mixture (4:1 v/v) and *temed* was added dropwise with stirring till a clear bluish green-coloured solution was obtained. The solution was allowed to evaporate slowly at room temperature and bluish-green shiny crystals of complex **1** started appearing after few days, which were separated from the mother liquor and dried in air. Complex **1** is soluble in methanol and DMSO and insoluble in water and decomposes at 157 °C. FT-IR (neat) (ν_{\max} , cm^{-1}): 3307(s), 3273(s), 3120(w), 2986(m), 2947(m), 1602(w), 1580(s), 1446(s), 1326(m), 1276(s), 1143(s), 1040(s), 760(s), 534(s), 473(m). UV-vis in DMSO, λ/nm ($\epsilon/\text{M}^{-1}\text{cm}^{-1}$): 660(85), 338(shoulder (sh)) (9800), 296 (20100). Anal. Calcd. for $\text{C}_{36}\text{H}_{44}\text{CuN}_4\text{O}_4$ (MW = 660.14): Cal. C, 65.44; H, 6.66; N, 8.48; Cu, 9.61 %; Found: C, 65.38; H, 6.72; N, 8.42; Cu, 9.54 %.

Synthesis of $[\text{Cu}(\text{en})_2(\text{H}_2\text{O})_2](\text{mef})_2$, **2.** Complex **2** was synthesized in a similar manner as complex **1** with the use of *en* instead of *temed* till a clear violet-colored solution was obtained. When the solution was allowed to evaporate slowly at room temperature, violet crystals appeared after a few days, which were separated from the mother liquor and dried in air. Complex **2** is soluble in methanol, DMSO, water and decomposes at 170 °C. The crystals for the complex obtained in good yield, i.e. 80 %. FT-IR (neat) (ν_{\max} , cm^{-1}): 3585(s), 3138(w), 2917(w), 1608(m), 1574(s), 1496(s), 1385(s), 1370(s), 1146(m), 1042(w), 1019(m), 672(m), 751(s), 718(s), 567(w), 524(m). UV-vis in DMSO, λ/nm ($\epsilon/\text{M}^{-1}\text{cm}^{-1}$): 620 (45), 340 (sh) (11000), 292 (19500). Anal. Calcd. for $\text{C}_{34}\text{H}_{48}\text{CuN}_6\text{O}_6$ (MW = 700.32): C, 58.26; H, 6.85; N, 11.99; Cu, 9.06 %; Found: C, 58.12; H, 7.05; N, 11.85; Cu, 8.97 %.

Synthesis of $[\text{Cu}(\beta\text{-pic})_2(\text{mef})_2\cdot\text{H}_2\text{O}$, **3.** Complex **3** was synthesized in a similar manner as complex **1** with the use of β -picoline instead of *temed* till a clear bluish green-colored solution was obtained. The solution was allowed to slow evaporation at room temperature, and dark green crystals suitable for determination of the structure with X-ray crystallography appeared after few days, which were separated from the mother liquor in good yield (76 %) and dried in air. Complex **3** is soluble in methanol and DMSO but insoluble in water and decomposes at 170 °C. FT-IR (neat) (ν_{\max} , cm^{-1}): 3217(m), 3064(w), 2941(m), 2860(w), 1609(s), 1575(s), 1364(s), 1151(m), 1064(w), 917(m), 794(s), 659(m), 569(m), 524(m), UV-Vis, λ/nm ($\epsilon/\text{M}^{-1}\text{cm}^{-1}$): in 4:1 (v/v) MeOH-H₂O: 747 (52), DMSO: 750 (80), 343 (11200), 288 (20500). Anal. Calcd. for $\text{C}_{42}\text{H}_{46}\text{CuN}_4\text{O}_5$ (MW = 748.32): C, 67.35; H, 6.14; N, 7.48; Cu, 8.48 %, Found: C, 65.97; H, 6.13; N, 7.14; Cu, 8.42 %.

Crystallography. Single-crystal X-ray diffraction data for complexes **2** and **3** were collected on a Nonius Kappa diffractometer equipped with a CCD detector with graphite-monochromatized MoK α radiation ($\lambda = 0.71069 \text{ \AA}$). Intensities were corrected for Lorentz, polarization and absorption effects.^[82] The structures were solved by direct methods with the SIR97 suite of programs^[83] and refinement was performed on F^2 by full-matrix least-squares methods with all non-hydrogen atoms anisotropic. In both structures, hydrogen atoms were included on calculated positions, riding on their

carrier atoms, apart from those belonging to water molecules or to NH group of mefenamate ion, that were found in the difference Fourier map and refined isotropically. In complex **3**, the elongated thermal ellipsoids of the N3-C27 ring and of the terminal methyl groups indicated possible disorder; however, efforts to model the disorder did not succeed in improving the reliability factors. The structure is reported without modeling the disorder. All calculations were performed using SHELXL-97^[84] implemented in the WINGX system of programs.^[85] Experimental details are given in reference [86].

DNA-binding studies by UV-Vis spectroscopy. The interaction of complexes **1-3** with CT DNA was studied by UV-Vis spectroscopy in order to investigate the possible binding modes to CT DNA and to calculate the DNA-binding constants (K_b). The UV-Vis spectra of CT DNA were recorded for a constant DNA concentration ($1.2\text{-}1.5 \times 10^{-4} \text{ M}$) in the presence of each complex at diverse [complex]/[DNA] mixing ratios ($= r$). The DNA-binding constant of the complexes (K_b , in M^{-1}) was determined by the Wolfe-Shimer equation (eq. S1)^[42] and the plots $[\text{DNA}]/(\epsilon_A - \epsilon_i)$ vs $[\text{DNA}]$ using the UV-Vis spectra of the complex recorded for a constant concentration ($3\text{-}5 \times 10^{-5} \text{ M}$) in the presence of DNA for diverse r values. Control experiments with DMSO were performed and no changes in the spectra of CT DNA were observed.

Cyclic voltammetry studies. Cyclic voltammograms of a 0.40 mM 1:2 DMSO:buffer solution of complexes **1-3** upon addition of DNA at diverse r values were complimentary used to evaluate the DNA-binding mode. The buffer was also used as the supporting electrolyte and the cyclic voltammograms were recorded at $v = 100 \text{ mV s}^{-1}$.

Viscosity measurements. The viscosity of DNA ($[\text{DNA}] = 0.1 \text{ mM}$) in buffer solution (150 mM NaCl and 15 mM trisodium citrate, pH 7.0) was measured in the presence of increasing amounts of complexes **1-3** (up to the value of $r = 0.35$). The obtained data are presented as $(\eta/\eta_0)^{1/3}$ versus r , where η is the viscosity of DNA in the presence of the compound and η_0 is the viscosity of free DNA in buffer solution. All measurements were performed at room temperature.

EB competitive studies with fluorescence emission spectroscopy. The competitive studies of complexes **1-3** with EB were monitored by fluorescence emission spectroscopy so as to investigate whether the complexes can displace EB from its DNA-EB conjugate. The DNA-EB compound was prepared by pre-treating 20 μM EB and 26 μM CT DNA in buffer (150 mM NaCl and 15 mM trisodium citrate at pH 7.0). The possible intercalating effect of the complexes was studied by adding stepwise a certain amount of a complex in solution into a solution of the DNA-EB complex till $r = 0.25$, and the fluorescence emission spectra were recorded with excitation wavelength at 540 nm. The complexes do not show any fluorescence emission band at room temperature in solution or in the presence of EB or CT DNA under the same experimental conditions; therefore, the observed quenching of the initial EB-DNA fluorescence may be assigned to the displacement of EB from its EB-DNA compound. The data are depicted as the percentage of EB-DNA (I/I_0 , %) fluorescence versus r . The Stern-Volmer constants (K_{SV} , in M^{-1}) have been calculated according to the linear Stern-Volmer equation (eq. S6)^[66] and the plots I_0/I vs $[Q]$.

Albumin-binding studies. The study of the binding of the complexes with serum albumins was performed by tryptophan

fluorescence emission quenching experiments using BSA (3 μM) or HSA (3 μM) in buffer (containing 15 mM trisodium citrate and 150 mM NaCl at pH 7.0). The quenching of the emission intensity of tryptophan residues of BSA at 343 nm or HSA at 352 nm was monitored using complexes **1-3** as quenchers with increasing concentration.^[60] The fluorescence emission spectra were recorded in the range 300–500 nm with an excitation wavelength of 295 nm. The fluorescence emission spectra of the free complexes were also recorded under the same experimental conditions, i.e. excitation at 295 nm and the compounds did not show any appreciable fluorescence emission band.^[40] Additionally, the influence of the inner-filter effect^[64] on the measurements was evaluated by eq. S3. The Stern-Volmer and Scatchard equations (eq. S4-S6)^[67] and graphs were used in order to calculate the dynamic quenching constant K_{SV} (in M^{-1}), the approximate quenching constant k_q (in $\text{M}^{-1}\text{s}^{-1}$), the SA-binding constant K (in M^{-1}) and the number of binding sites per albumin.

Acknowledgement. The authors gratefully acknowledge the financial support of UGC, New Delhi (India) as UGC Emeritus (RPS) and BSR (SK) fellowships. The DFT computations were performed (MW) using computers of the Wrocław Centre for Networking and Supercomputing Grant No. 47.

Notes and references

- G.C. Seuanes, M.B. Moreira, T. Petta, M.P.D. Lama, L.A.B. de Moraes, A.R.M. de Oliveira, R.M. Zumstein, G. Naal and S. Nikolaou, *J. Inorg. Biochem.* 2015, **153**, 178.
- G. Ribeiro, M. Benadiba, A. Colquhoun and D.O. Silva, *Polyhedron* 2008, **27**, 1131.
- D.O. Silva, *Med. Chem.* 2010, **10**, 3122.
- A. Herwadkar, V. Sachdeva, L.F. Taylor, H. Silver and A.K. Banga, *Int. J. Pharm.* 2012, **423**, 289.
- M. Edrissi, N. Razzaghi and B. Madjidi, *Turk. J. Chem.* 2008, **32**, 505.
- F.T. Greenaway, E. Riviere, J.J. Girerd, X. Labouze, G. Morgant, B. Viossat, J.C. Daran, M. N. RochArveiller and H. Dung, *J. Inorg. Biochem.* 1999, **76**, 19-27.
- J. Moncol, B. Kalinakova, J. Svorec, M. Kleinova, M. Koman, D. Hudecova, M. Melnik, M. Mazur and M. Valko, *Inorg. Chim. Acta.* 2004, **357**, 3211.
- S. Dutta, S. Padhye and V. McKee, *Inorg. Chem. Commun.* 2004, **7**, 1071.
- E.R.T. Tiekink, *Trend Organomet. Chem.* 1994, **9**, 71.
- G. Prabusankar and R. Murugavel, *Organometallics* 2004, **2**, 5644.
- G. Crisponi, V.M. Nurchi, D. Fanni, C. Gerosa, S. Nemolato and G. Faa, *Coord. Chem. Rev.* 2010, **254**, 876.
- M. Ruiz, L. Perello, J. Server-Carrio, R. Ortiz, S. Garcia-Granda, M.R. Diaz and E. Canton, *J. Inorg. Biochem.* 1998, **69**, 231.
- A.M. Ramadan, *J. Inorg. Biochem.* 1997, **65**, 183.
- C. Santini, M. Pellei, V. Gandin, M. Porchia, F. Tisato and C. Marzano, *Chem. Rev.* 2014, **114**, 815.
- J.R.J. Sorenson and H. Sigel, *Metal Ions in Biological system*, 1982, Marcel Dekker, New York, **14**, 77.
- V. Dokorou, Z. Ciunik, U. Russo and D. Kovala-Demertzi, *J. Organomet. Chem.* 2001, **630**, 205.
- C. Nunes, G. Brezesinski, J.L.F.C. Lima, S. Reis and M. Lucio, *J. Phys. Chem. B* 2011, **115**, 8024.
- J.E. Weder, C.T. Dillon, T.W. Humbley, B.J. Kennedy, P.A. Lay, J.R. Biffin, H.L. Regtop and N.M. Davies, *Coord. Chem. Rev.* 2002, **232**, 95.
- L.W. Oberley, G. R. Buettner, *Cancer Research* 1979, **39**, 1141.
- R. Bregier-Jarzebowska A. Gasowska, S.K. Hoffmann, L. Lomozik. *J. Inorg. Biochem.* 2016, in press doi:10.1016/j.jinorgbio.2016.06.007
- A. Ozarowski, C.J. Calzado, R.P. Sharma, S. Kumar, J. Jezierska, C. Angeli, F. Spizzo and V. Ferretti, *Inorg. Chem.* 2015, **54**, 11916
- A. Saini, R.P. Sharma, S. Kumar, P. Venugopalan, P. Starynowicz and J. Jezierska. *Inorg. Chim. Acta.* 2015, **436**, 169.
- S. Kumar, R.P. Sharma, P. Venugopalan, J. Jezierska, A. Wojciechowska and V. Ferretti, *Inorg. Chim. Acta.* 2015, **432**, 221.
- A. Saini, R.P. Sharma, S. Kumar, P. Venugopalan, A.I. Gubanov and A. Smolentsev, *Polyhedron* 2015, **100**, 155.
- L.J. Bellamy, *The Infrared Spectra of Complex Molecules*, Chapman & Hall London/New York, second ed., 1980.
- K. Nakamoto, *Infrared and Raman Spectra of Inorganic and Coordination Compounds*, John Wiley & Sons, New York, fifth ed., 1997.
- W. Brzyska and W. Ozga, *Pol. J. Chem.* 1993, **67**, 619.
- A. Topaclı, S. Lde and J. Pharm. *Biomed. Anal.* 1999, **21**, 975.
- R.C. Mehrotra and R. Bohra, *Metal Carboxylates*, Academic Press Inc. London, 1983.
- N. Ahmad, A.H. Chughtai, H.A. Younus and F. Verpou, *Coord. Chem. Rev.* 2014, **280**, 1.
- N.E. Brese and M. O'Keeffe, *Acta Crystal.* 1991, **B37**, 431.
- F. Jiang, K. D. Karlin and J. Peisach, *Inorg. Chem.* 1993, **32**, 2576.
- B. Kozlevcar, A. Golobic and P. Strauch, *Polyhedron* 2006, **25**, 2824.
- J. Peisach and W. E. Blumberg, *Arch. Biochem. Biophys.* 1974, **165**, 691.
- G. Plesch, C. Friebel, O. Svajlenova and J. Kratsmar-Smogrovic, *Polyhedron* 1995, **14**, 1185.
- G. Plesch, C. Friebel, S.A. Warda, J. Sivy and O. Svajlenova, *Trans. Met. Chem.* 1997, **22**, 433.
- W.J. Geary, *Coord. Chem. Rev.* 1971, **7**, 81.
- B.M. Zeglis, V.C. Pierre and J.K. Barton, *Chem. Commun.* 2007, 4565.
- G. Pratiel, J. Bernadou and B. Meunier, *Adv. Inorg. Chem.* 1998, **45**, 251.
- F. Dimiza, A.N. Papadopoulos, V. Tangoulis, V. Psycharis, C.P. Raptopoulou, D.P. Kessissoglou and G. Psomas, *Dalton Trans.* 2010, **39**, 4517.
- F. Dimiza, S. Fountoulaki, A.N. Papadopoulos, C.A. Kontogiorgis, V. Tangoulis, C.P. Raptopoulou, V. Psycharis, A. Terzis, D.P. Kessissoglou and G. Psomas, *Dalton Trans.* 2011, **40**, 8555.
- A. Tarushi, Z. Karafliou, J. Kljun, I. Turel, G. Psomas, A.N. Papadopoulos and D.P. Kessissoglou, *J. Inorg. Biochem.* 2013, **128**, 85.
- a) X. Totta, A.A. Papadopoulou, A.G. Hatzidimitrou, A. Papadopoulos and G. Psomas, *J. Inorg. Biochem.* 2015, **145**, 79; b) S. Tsiliou, L.-A. Kefala, A.G. Hatzidimitriou, D.P. Kessissoglou, F. Perdih, A.N. Papadopoulos, I. Turel and G. Psomas, *J. Inorg. Biochem.*, 2016, **160**, 125.
- A. Wolfe, G. Shimer and T. Meehan, *Biochemistry* 1987, **26**, 6392.
- G. Psomas and D.P. Kessissoglou, *Dalton Trans.* 2013, **42**, 6252.
- A. Dimitrakopoulou, C. Dendrinou-Samara, A.A. Pantazaki, M. Alexiou, E. Nordlander and D.P. Kessissoglou, *J. Inorg. Biochem.* 2008, **102**, 618.
- F. Dimiza, F. Perdih, V. Tangoulis, I. Turel, D.P. Kessissoglou and G. Psomas, *J. Inorg. Biochem.* 2011, **105**, 476.
- C. Tolia, A.N. Papadopoulos, C.P. Raptopoulou, V. Psycharis, C. Garino, L. Salassa and G. Psomas, *J. Inorg. Biochem.* 2013, **123**, 53.

49. A. Tarushi, C.P. Raptopoulou, V. Psycharis, D.P. Kessissoglou, A.N. Papadopoulos and G. Psomas, *J. Inorg. Biochem.*, 2014, **140**, 185.
50. A. Tarushi, S. Perontsis, A.G. Hatzidimitriou, A.N. Papadopoulos, D.P. Kessissoglou and G. Psomas, *J. Inorg. Biochem.* 2015, **149**, 68.
51. M. Zampakou, N. Rizeq, V. Tangoulis, A.N. Papadopoulos, F. Perdihi, I. Turel and G. Psomas, *Inorg. Chem.* 2014, **53**, 2040.
52. a) M. Zampakou, V. Tangoulis, C.P. Raptopoulou, V. Psycharis, A.N. Papadopoulos and G. Psomas, *Eur. J. Inorg. Chem.* 2015, 2285; b) S. Perontsis, A.G. Hatzidimitriou, O.-A. Begou, A.N. Papadopoulos and G. Psomas, *J. Inorg. Biochem.* 2016, **162**, 22; c) S. Perontsis, A.G. Hatzidimitriou, A.N. Papadopoulos and G. Psomas, *J. Inorg. Biochem.* 2016, **162**, 9; d) A. Tarushi, C.P. Raptopoulou, V. Psycharis, C.K. Kontos, D.P. Kessissoglou, A. Scorialas, V. Tangoulis and G. Psomas, *Eur. J. Inorg. Chem.* 2016, 219.
53. A. Tarushi, X. Totta, A. Papadopoulos, J. Kljun, I. Turel, D.P. Kessissoglou and G. Psomas, *Eur. J. Med. Chem.* 2014, **74**, 187.
54. A. Jancso, L. Nagy, E. Moldrheim and E. Sletten, *J. Chem. Soc. Dalton Trans.* 1999, 1587.
55. M.T. Carter, M. Rodriguez and A.J. Bard, *J. Am. Chem. Soc.* 1989, **111**, 8901.
56. G. Psomas, *J. Inorg. Biochem.* 2008, **102**, 1798.
57. P. Zivec, F. Perdihi, I. Turel, G. Giester and G. Psomas, *J. Inorg. Biochem.* 2012, **117**, 35.
58. D. Li, J. Tian, W. Gu, X. Liu and S. Yan, *J. Inorg. Biochem.* 2010, **104**, 171.
59. J. L. Garcia-Gimenez, M. Gonzalez-Alvarez, M. Liu-Gonzalez, B. Macias, J. Borrás and G. Alzuet, *J. Inorg. Biochem.* 2009, **103**, 923.
60. J.R. Lakowicz, *Principles of Fluorescence Spectroscopy*, third ed. Plenum Press, New York, 2006.
61. W.D. Wilson, L. Ratmeyer, M. Zhao, L. Strekowski and D. Boykin, *Biochemistry* 1993, **32**, 4098.
62. G. Zhao, H. Lin, S. Zhu, H. Sun and Y. Chen, *J. Inorg. Biochem.* 1998, **70**, 219.
63. C. Tan, J. Liu, H. Li, W. Zheng, S. Shi, L. Chen and L. Ji, *J. Inorg. Biochem.* 2008, **102**, 347.
64. L. Stella, A.L. Capodilupo and M. Bietti, *Chem. Commun.* 2008, 4744.
65. V. Rajendiran, R. Karthik, M. Palaniandavar, H. Stoeckli-Evans, V.S. Periasamy, M.A. Akbarsha, B.S. Srinag and H. Krishnamurthy, *Inorg. Chem.* 2007, **46**, 8208.
66. G. Zhao, H. Lin, S. Zhu, H. Sun and Y. Chen, *J. Inorg. Biochem.* 1998, **70**, 219.
67. Y. Wang, H. Zhang, G. Zhang, W. Tao and S. Tang, *J. Luminescence* 2007, **126**, 211.
68. O.H. Laitinen, V.P. Hytonen, H.R. Nordlund and M.S. Kulomaa, *Cell. Mol. Life Sci.* 2006, **63**, 2992.
69. R. Xu, W. Pang and Q. Huo, *Modern inorganic synthetic chemistry*, Elsevier, 2011.
70. M.A. Malati, *Experimental Inorganic Chemistry*, first ed., Harwood Publishing, Chichester, 1999.
71. F. Neese, *Wiley Interdiscip. Rev. Comput. Mol. Sci.* 2012, **2**, 73.
72. A. D. Becke, *J. Chem. Phys.* 1993, **98**, 5648.
73. C. Lee, W. Yang and R.G. Parr, *Phys. Rev. B* 1988, **37**, 785.
74. P.J. Stephens, F.J. Devlin, C.F. Chabalowski and M.J. Frisch, *J. Phys. Chem.* 1994, **98**, 11623.
75. C. van Wuellen, *J. Chem. Phys.* 1998, **109**, 392.
76. D.A. Pantazis, X.Y. Chen, C.R. Landis and F. Neese, *J. Chem. Theor. Comput.* 2008, **4**, 908.
77. F. Neese, *J. Chem. Phys.* 2001, **115**, 11080.
78. F. Neese, *J. Chem. Phys.* 2005, **122**, 34107.
79. F. Neese, F. Wennmohs, A. Hansen and U. Becker, *Chem. Phys.* 2009, **356**, 98.
80. J. Marmur, *J. Mol. Biol.*, 1961, **3**, 208.
81. M.F. Reichmann, S.A. Rice, C.A. Thomas and P. Doty, *J. Am. Chem. Soc.* 1954, **76**, 3047.
82. R.H. Blessing, *Acta Crystallogr.* 1995, **A51**, 33.
83. A. Altomare, M.C. Burla, M. Camalli, G. Cascarano, C. Giacovazzo, A. Guagliardi, A.G. Moliterni, G. Polidori and R. Spagna, *J. Appl. Crystallogr.* 1999, **32**, 115.
84. G.M. Sheldrick, *SHELXL97, Program for Crystal Structure Refinement*, University of Göttingen, Germany, 1997.
85. L. J. Farrugia, *J. Appl. Crystallogr.* 1999, **32**, 837.
86. **Crystal Data for Complex 2:** $M_r = 700.32 \text{ g mol}^{-1}$, triclinic, space group $P1\bar{1}$; $a = 7.6611(4) \text{ \AA}$, $b = 7.7237(4) \text{ \AA}$, $c = 17.5068(10) \text{ \AA}$; $\alpha = 79.714(3)^\circ$, $\beta = 83.229(3)^\circ$, $\gamma = 61.736(3)^\circ$; $V = 897.08(9) \text{ \AA}^3$; $Z = 1$; 4278 independent reflections ($R_{\text{int}} = 0.058$), $R1 = 0.043$, $wR2 = 0.114$, $S = 1.08$. $R1$ was calculated for observed data and $wR2$ for all data.
- Crystal Data for Complex 3:** $M_r = 1496.70 \text{ g mol}^{-1}$, triclinic, space group $P1\bar{1}$; $a = 11.2953(5) \text{ \AA}$, $b = 11.3767(6) \text{ \AA}$, $c = 16.1337(7) \text{ \AA}$; $\alpha = 93.629(3)^\circ$, $\beta = 99.882(3)^\circ$, $\gamma = 108.993(3)^\circ$; $V = 1915.41(16) \text{ \AA}^3$; $Z = 1$; 8261 independent reflections ($R_{\text{int}} = 0.096$), $R1 = 0.067$, $wR2 = 0.200$, $S = 1.05$. $R1$ was calculated for observed data and $wR2$ for all data.

The interaction of three newly synthesized copper(II) mefenamate complexes with bovine/human serum albumin was studied by fluorescence emission spectroscopy.

